Magnet design studies for RACCAM

Bruno Autin* and Emmanuel Froidefond†

*CERN, Geneva - Bruno.Autin@cern.ch
†Laboratoire de Physique Subatomique et de Cosmologie, 53 avenue des martyrs, 38026 Grenoble Cedex - emmanuel.froidefond@lpsc.in2p3.fr

Abstract. In the frame of the *RACCAM* project, possible of designs of a spiral FFAG for medical applications are studied. The main magnets used are dipoles with spiral edges. The magnetic field the has to follow the law $B_0\,(r/r_0)^k$. The magnet design studies has to include the possibility of a variable k to make easier variable extraction energy. The aim of this study is then to build a Mathematica function that allow the calculation of current intensities in the conductors distributed on the poles. The function is simply based on the Biot and Savart law. Then the matrix system $A \cdot I = B$ is deduced and lead to a solution vector B if A is well conditioned. Different configurations were tested with POISSON and gave good results. Different configurations were tested with POISSON and gave good results.. Different configurations were tested with POISSON and gave good results.

Keywords: RACCAM, magnet design, conductor distribution, Mathematica

INTRODUCTION

In the frame of the *RACCAM* project, the design of a spiral FFAG for medical application is studied to allow a higher repetition rate, fast acceleration and quick extraction energy variation. The magnetic field law is non linear and writes as follow :

$$B(r,\zeta) = B_0 \left(\frac{r}{r_0}\right)^k \tag{1}$$

.

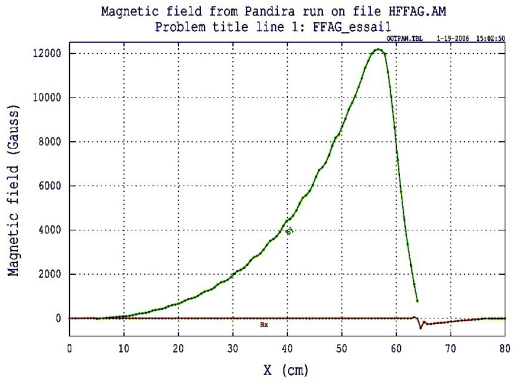

FIGURE 1. *POISSON* simulation of $B_y(r)$ with the KURRI spiral injector geometry.

One can obtain a similar magnetic field law using the current law $I_0\,(r/r_0)^k$. But, in this particular case, the k value of the current law is completely different from the one of $B_y(r)$. The magnetic field shown in fig.1 follows $B_y(r)$, calculating the contribution of each conductor in the median plane and using for that the Biot and Savart law. The calculations of this study where leaded with the geometry of the KURRI-ADS spiral injector dipoles (see fig. 2). If the number of observation is limited, then the field law is generated with a matrix system of the form $A \cdot I = B$.

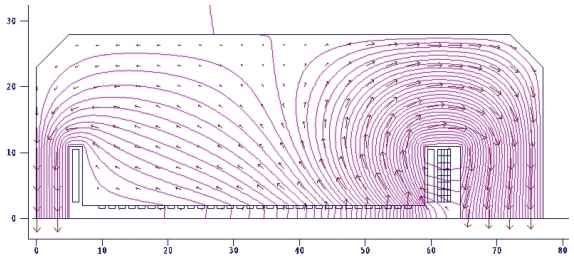

FIGURE 2. The KURRI spiral injector geometry with field lines.

With such a geometry, the field oscillations (that can be already seen on fig.1) are unavoidable as shown in fig.3.

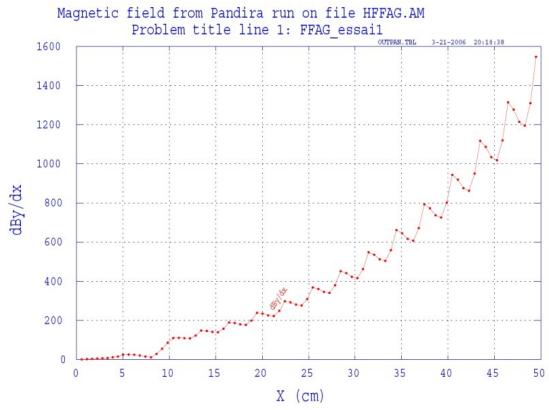

FIGURE 3. The KURRI spiral injector geometry with field lines.

FIELD PRODUCED BY A DISTRIBUTION OF CONDUCTORS

Current Intensities Calculation

Field Components For A Series Of Conductors

Let the conductor coordinates be $\{\xi,\eta\}$, the Biot and Savart law gives the field components at the observation $\{x,0\}$ in the median plane :

$$B_x(x,\xi,\eta)=\frac{\mu_0 I}{4\pi}\frac{\eta}{(x-\xi)^2+\eta^2} \tag{2}$$

$$B_y(x,\xi,\eta)=\frac{\mu_0 I}{4\pi}\frac{x-\xi}{(x-\xi)^2+\eta^2} \tag{3}$$

Now, consider a series of N conductors. The field components then become :

$$B_x(x,\xi_i,\eta_i)=\frac{\mu_0}{4\pi}\sum_N^{i=1} I_i\frac{\eta_i}{(x-\xi_i)^2+\eta_i^2} \tag{4}$$

$$B_y(x,\xi_i,\eta_i)=\frac{\mu_0}{4\pi}\sum_N^{i=1} I_i\frac{x-\xi_i}{(x-\xi_i)^2+\eta_i^2} \tag{5}$$

Magnetic Field In The Median Plane

Now consider a series of P observation points, the magnetic field is then represented as a series of magnetic field values. The field components are then written as follow :

$$B_{x,y}(\{x_j\},\{\xi_i,\eta_i\})=\begin{pmatrix} B_{x,y1}(x_1,\{\xi_i,\eta_i\}) \\ B_{x,y2}(x_2,\{\xi_i,\eta_i\}) \\ \vdots \\ B_{x,yP}(x_P,\{\xi_i,\eta_i\}) \end{pmatrix}$$

The distribution of current intensities is then built as a vector :

$$I=\begin{pmatrix} I_1 \\ I_2 \\ \vdots \\ I_N \end{pmatrix}$$

So the whole system is reduced to a simple matrix equation :

$$A_{x,y}\cdot I=B_{x,y} \tag{6}$$

where A is composed of components as those of equations (4) and (5) :

$$A_x=\begin{pmatrix} \frac{\eta_1}{(x_1-\xi_1)^2+\eta_1^2} & \cdots & \frac{\eta_N}{(x_1-\xi_N)^2+\eta_N^2} \\ \vdots & \ddots & \vdots \\ \frac{\eta_1}{(x_P-\xi_1)^2+\eta_1^2} & \cdots & \frac{\eta_N}{(x_P-\xi_N)^2+\eta_N^2} \end{pmatrix}$$

or

$$A_y=\begin{pmatrix} \frac{x_1-\xi_1}{(x_1-\xi_1)^2+\eta_1^2} & \cdots & \frac{x_1-\xi_1}{(x_1-\xi_N)^2+\eta_N^2} \\ \vdots & \ddots & \vdots \\ \frac{x_P-\xi_1}{(x_P-\xi_1)^2+\eta_1^2} & \cdots & \frac{x_P-\xi_N}{(x_P-\xi_N)^2+\eta_N^2} \end{pmatrix}.$$

Matrices A_x and A_y have the dimensions $P\times N$. As it will be seen in the following subsection, the number of observation points P is chosen to be greater than the number of conductors N for calculation precision reasons. It follows that the number of unknowns is greater than the number of linear equations. That makes the system overdetermined. The first simple idea to get rid of this problem is to use the transpose matrix $A^T_{x,y}$. The equation (6) then becomes :

$$A^T_{x,y}\cdot A_{x,y}\cdot I=A^T_{x,y}\cdot B_{x,y} \tag{7}$$

This equation is then easily solved using common *Mathematica* programming.

Application Of The Matrix Equation To The KURRI Spiral Dipole Geometry

Current calculation with the Mathematica function

The injector has an energy range different from that of the RACCAM's FFAG designs. The minimum and maximum magnetic field, corresponding respectively to injection and extraction, are then bigger with such values as 0.1 T and 1.8 T. The gap height is 40 mm and the radial extent 0.465 m. The number of conductors is 32 on one pole.

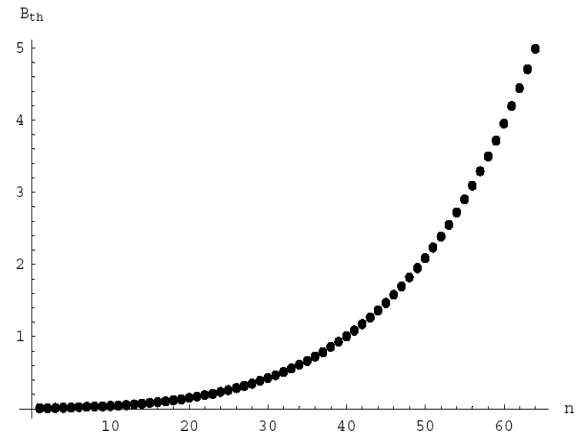

FIGURE 4. n is the number of conductors of the model. Original field law is given by conductors between n=16 and n=48.

As border conditions are not taken into account, the solution has oscillating values, up to unrealistic values

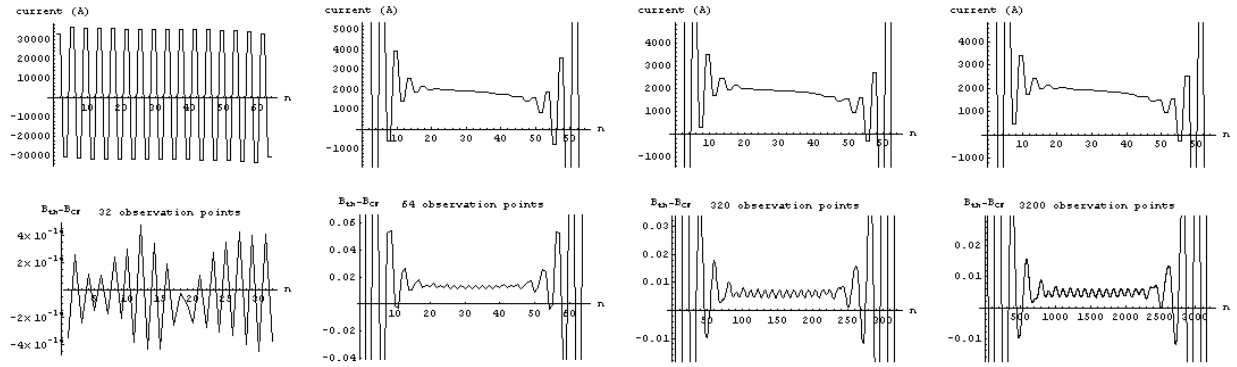

FIGURE 5. 32 conductors case with P varying from 32 to 3200. The current intensities has to be divided by two to coarsely take into account the effect of iron.

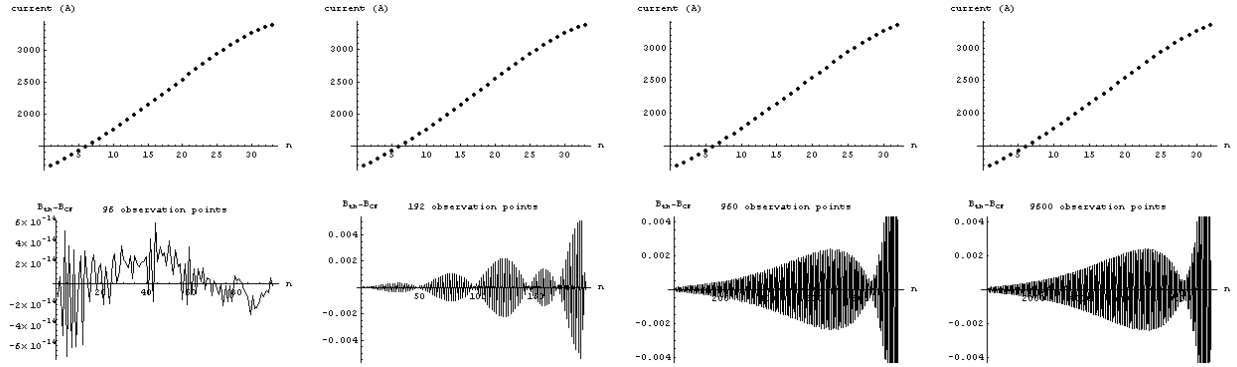

FIGURE 6. 96 conductors case with P varying from 96 to 9600. The current intensities has to be divided by two to coarsely take into account the effect of iron.

for one dipole as 150000A in the worst case with 32 conductors in a half plane (see fig.5). In this case, the model radial extent is equal to the "good field region" length $l_{gfr} = 0.465$m, and whatever is the number of observation points, the precision of the calculated field B_{cf} is is equal or greater than 0.5%.
This problem can be avoided by increasing the radial extent of the model. The field calculated in the region of interest can reach the machine precision with a radial extent of $3l_{gfr}$ (see fig.6).

POISSON *simulations*

The current calculated with the Mathematica function are now applied to the KURRI spiral injector geometry. *POISSON* simulations show that the conductor are not able to produce the field law correctly. The field law is translated to low values, such that low field values are negative (see fig.7).

To correct this, A uniform field of empirical intensity is added (see fig1).

FIELD PRODUCED BY A PROFILED CONDUCTING LAYER

To avoid field oscillations, it is logical to imagine a conducting layer that covers the whole surface of the pole, with a varying thickness. As a consequence, the current density is constant, and the dipole powering is simplified with one conductor for one magnet. To match the desired field law the constraint parameter is the conductor thickness $h(\xi)$. After the integration over η, the field components now read :

$$B_x(x,\xi,\eta) = \int \left(\arctan\left[\frac{g}{x-\xi}\right] + \arctan\left[\frac{h[\xi]}{x-\xi}\right] \right) d\xi \qquad (8)$$

$$B_y(x,\xi,\eta) = \frac{1}{2}\int \left(\log[g^2 + (x_\xi)^2] - \log[h[\xi]^2 + (x-\xi)^2] \right) d\xi \qquad (9)$$

The main advantage of this solution is the high field gradient values achievable. This is due to the possibility

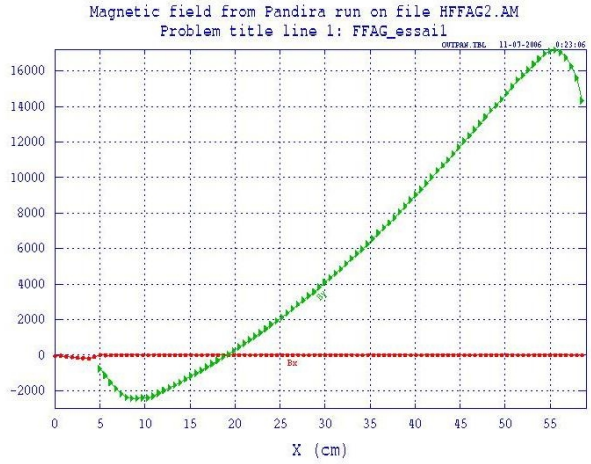

FIGURE 7. Field law calculated with *POISSON* (in Gauss) using currents calculated with the model of $3l_{gfr}$ radial extent.

to set the thickness of the layer to such values that the current density at radius r can be very high.

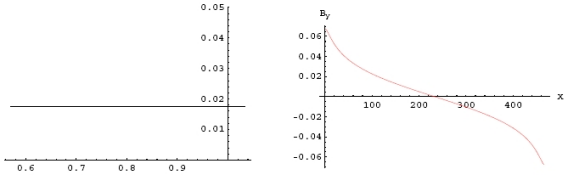

FIGURE 8. Field law calculated for a conducting layer of constant thickness.

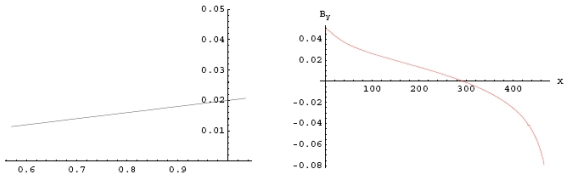

FIGURE 9. Field law calculated for a conducting layer of linearly decreasing thickness (e.g. for constant focusing).

FIELD PRODUCED BY CONDUCTING STRIPES

Even if a conducting layer erase field oscillations, it is not applicable to variable k FFAGs. To decrease the amplitude of oscillations, the pole can be covered by conducting stripes (no free space between conductors). That allow a variable k in the same way as the conductors of the KURRI spiral injector geometry do.

Matrix Construction For Stripes

The field component then only depend on the integration over ξ. If a stripe radial width is comprised between abscissa p_i and q_i, the components of matrix $A_{x,y}$ should be written as this : $\int_{p_i}^{q_i} f_i(x_j,\xi)d\xi$. But, in order to take into account the possibility to have stripe of different thickness, the calculation includes the integration over η from $h[\xi]$ to g. This can be used for example in linear shaping to obtain a constant focusing of a spiral dipole.

$$A_{x,y} = \begin{pmatrix} \int_{p_1}^{q_1}\int f(x_1,\xi)d\eta d\xi & \cdots & \int_{p_N}^{q_N}\int f(x_1,\xi)d\eta d\xi \\ \vdots & \ddots & \vdots \\ \int_{p_1}^{q_1}\int f(x_P,\xi)d\eta d\xi & \cdots & \int_{p_N}^{q_N}\int f(x_P,\xi)d\eta d\xi \end{pmatrix}$$

After integration over η, the elements of the matrix have the same form as in equations 8 and 9. A calculation in the case of the KURRI spiral injector geometry (constant thickness and constant gap) results in the same current values as those of thin conductors (second section). A numerical simulation with *POISSON* (see fig.10) shows lower field oscillations comparing it to thin conductors case (see fig.3. The influence now has to be tested on particle tracking, so that a choice could be done concerning the type of conductors geometry.

Thin Stripes Extent

In the case of stripe thickness very small compared to the gap height, two main advantages appear :

1. the thickness disappear from the horizontal component :
   $B_{x,j}(x,\xi) =$
   $\frac{1}{2}\left(-2\arctan\left[\frac{x-\xi}{g}\right]-(x-\xi)\log\left[\frac{(x-\xi)^2+g^2}{(x-\xi)^2}\right]\right)$,

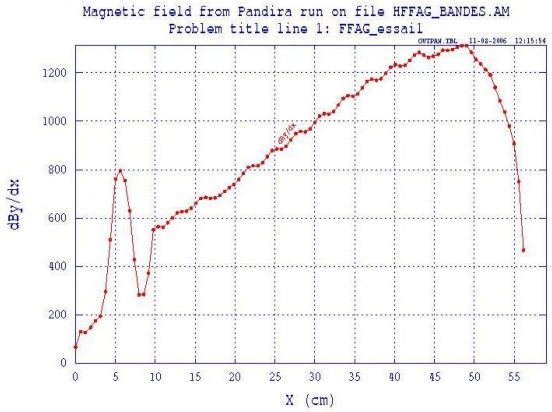

FIGURE 10. Field oscillations with stripe conductors, with thickness and gap height from the KURRI spiral injector geometry.

2. the vertical component integral has now a linear dependence on thickness :
   $B_{y,j}(x,\xi) = \int -\frac{(x-\xi)h[\xi]}{(x-\xi)^2+g^2} d\xi.$

For the integration of the vertical component, two main cases appear :

1. $h[\xi]$ has any expression : the integration is numerical,
2. $h[\xi]$ has a polynomial expression : the integration can be analytical.

CONCLUSION

A set of *Mathematica* functions has been written that allow to produce current intensities calculations for arrays of conductors distributed on the poles of a dipole, for three types of conductor geometry. They have been tested on simple cases and gave good results. Solutions are given to diminish or totally get rid of field oscillations with conductor shaping or stripe conductors. A good agreement was found between thin conductors and stripes.But these function and has to tested further more on more difficult geometries. For example in the case of a dipole with a large radial extent compared to the gap height, it has been seen that the precision of the calculation has to be increased. Several matrix parameters show that $A_{x,y}$ is ill-conditioned if the model is not defined carefully. Then, colleagues from the RACCAM project calculated the current intensities by other means, and found completely different intensities for magnetic fields of the same order of magnitude.

ACKNOWLEDGMENTS

We want to acknowledge our Japanese colleagues to allow us to use their data to test our calculations. We were also very pleased of the helpful discussions on magnet design and the kindness of Japanese welcoming.

REFERENCES

1. Y. Ishi, "Accelerator design and construction for FFAG-KUCA ADSR", presentation, Oct. 15th 2004.
2. X. Maréchal, J. Chavanne, P. Elleaume, "On 2-D periodic magnetic field", ESRF report ESRF-SR/ID-90-38, April 1990

REFERENCES